Proceedings of the
9th Graz Brain-Computer Interface Conference 2024
10.3217/978-3-99161-014-4-041

ASSESSING CALIBRATION DURATIONS FOR C-VEP-BASED BCIS: INSIGHTS FROM NON-BINARY PATTERNS AND SPATIAL FREQUENCY VARIATIONS

V. Martínez-Cagigal[1, 2], Á. Fernández-Rodríguez[3], E. Santamaría-Vázquez[1, 2], A. Martín-Fernández[1], R. Hornero[1, 2]

[1]Biomedical Engineering Group, University of Valladolid, Valladolid, Spain
[2]Centro de Investigación Biomédica en Red de Bioingeniería, Biomateriales y Nanomedicina (CIBER-BBN), Valladolid, Spain
[3]UMA BCI Group, University of Malaga, Malaga, Spain

E-mail: victor.martinez.cagigal@uva.es

ABSTRACT: BCIs using code-modulated visual evoked potentials (c-VEP) have become popular for their reliable, high-speed control of applications and devices. However, traditional circular shifting paradigms based on black & white stimuli can cause eyestrain for some users. We previously showed that adjusting the number of code events and spatial frequency can enhance user comfort. Despite c-VEP calibration being notably shorter than other BCIs, the optimal number of calibration cycles for effective system control remains unexplored. This study aims to investigate the impact of calibration duration on various c-VEP-based BCIs, with stimulus variations to improve user experience. We evaluated performance with different calibration cycles using five *p*-ary m-sequences encoded with shades of gray and eight spatial frequency variations of checkerboard-like stimuli. Results indicate that all conditions achieved over 90% accuracy and 80 bpm with calibration durations ranging between 6–70 seconds. These findings highlight the importance of selecting a configuration based on the functional requirements of the BCI.

INTRODUCTION

Non-invasive brain-computer interface (BCI) systems enable users to control external applications or devices by processing their electroencephalographic (EEG) activity in real-time [1]. However, direct interpretation of users' intentions from EEG signals is not feasible, making necessary to rely on task-based paradigms that elicit specific control signals. These paradigms encompass strategies that induce measurable deflections in the EEG during cognitive tasks or the processing of external stimuli, such as visual flashes [1]. Among such approaches, code-modulated visual evoked potentials (c-VEPs) have gained popularity in recent years due to their ability to achieve high-performance BCIs with short calibration times.

Traditional c-VEP-based BCIs utilize flickering stimuli generated by pseudorandom binary codes that shows perfect autocorrelation properties [2]. These time series encode selectable commands using temporally shifted versions of the same code. Calibration in this paradigm, known as circular shifting, typically requires extracting the brain response elicited by the original code over the primary visual cortex as a template. It is assumed that the response to subsequent commands corresponds to temporally shifted versions of this template according to each command's lag [2]. Thus, the main advantage of the circular shifting paradigm is that calibration is drastically reduced by estimating the brain response to a single sequence, independently of the total number of commands. Despite the excellent performance of high-contrast flickering produced by binary codes, which encode commands with black and white flashes, several studies have highlighted potential issues such as visual eyestrain and fatigue among certain users [3, 4]. One of the current areas of research in the state-of-the-art is focused on improving users' comfort without compromising performance. Previous studies have shown that this goal can be achieved through various methods, such as increasing the stimulation rate [5], employing customized codes that confine spectral density to high-frequency bands [6], using sequences with a high number of events allowing encoding with different shades of gray rather than high-contrast stimuli [5], or increasing the spatial frequency of checkerboard-like stimuli [7]. Specifically, we have previously demonstrated in studies by Martínez-Cagigal *et al.* (2023) [5] and Fernández-Rodríguez *et al.* (2023) [7] that these two latter approaches effectively enhance user comfort while maintaining similar levels of accuracy and information transfer rate (ITR).

In comparison with other systems, such as those based on P300 potentials or sensorimotor rhythms, c-VEP-based BCIs require notably fewer calibration trials. Nevertheless, some authors have proposed adaptive algorithms to further reduce or completely eliminate the need for calibration. For example, Spüler *et al.* (2013) [8] introduced an unsupervised clustering-based approach with two calibration targets, Thielen *et al.* (2021) [9] presented an adaptive version of "reconvolution" tailored for

Published by
Verlag der Technischen Universität Graz

10.3217/978-3-99161-014-4-041

zero-shot calibration contexts, and Stawicki & Volosyak (2022) [10] explored the potential of transfer learning to minimize recalibration across multiple sessions.

In spite of the increasing popularity of c-VEPs in non-invasive BCIs, to our knowledge, no study has specifically investigated the number of calibration cycles needed to effectively control the system. Consequently, this has not been explored for stimulus modifications aimed at enhancing user experience either. Therefore, the aim of this study is to analyze the impact of calibration duration in circular shifting c-VEP paradigms. Specifically, we examine typical binary black and white stimuli, *p*-ary m-sequences encoded with different shades of gray, and variations of spatial frequencies in checkerboard patterns.

SUBJECTS

In this study, we utilized data from two previously recorded databases [5, 7]. In both databases, all aspects of BCI operation were managed using open-source applications of MEDUSA©, accessible at medusabci.com [11]. Visual stimuli were presented on an LED FullHD @ 144 Hz monitor (model: KEEP OUT XGM24F+ 23.8") with a refresh rate of 120 Hz. EEG signals were registered using a g.USBamp device (g.Tec, Guger Technologies, Austria) from 16 active Ag/AgCl channels at positions F3, Fz, F4, C3, Cz, C4, CPz, P3, Pz, P4, PO7, POz, PO8, Oz, I1, and I2, according to the International System 10/5. The device was grounded at AFz and referenced to the right earlobe. All participants provided informed consent before participating [5, 7].

P-ary m-sequences database: This dataset comprises 15 healthy participants (aged 28.80 $\pm$ 5.02 years, 10 males, 5 females) [5] who engaged in BCI spelling tasks using the open-source "P-ary c-VEP Speller" application of MEDUSA©, accessible at medusabci.com/market/pary_cvep [11]. Participants completed a single session consisting of a calibration phase comprising 300 cycles and an online spelling task comprising 32 trials (with 10 cycles per trial) for each *p*-ary m-sequence. A total of five *p*-ary m-sequences were assessed: binary GF(2^6) with a base of 2, GF(3^5) with a base of 3, GF(5^3) with a base of 5, GF(7^2) with a base of 7, and GF(11^2) with a base of 11. Events were encoded using various shades of gray; e.g., GF(2^6) employed black and white flashes, while GF(5^3) used three equidistant grey tones in addition to black and white flashes, and so forth. Figure 1(A) illustrates all *p*-ary m-sequences, along with the arrangement of commands' lags. Online selections were made using a 4×4 command matrix (chance level of 6.25%), comprising alphabetic characters from A to P. For further details, please see Martínez-Cagigal *et al.* (2023) [5].

Checkerboard database: This dataset comprises 16 healthy participants (aged 29.63 $\pm$ 4.06 years, 11 males, 5 females) [7] who undertook BCI spelling tasks using a modified version of the open-source "c-VEP Speller" application provided by MEDUSA©, accessible at medusabci.com/market/cvep_speller [11]. Participants completed a single session, which included a calibration phase consisting of 300 cycles and an online spelling task comprising 18 trials (with 8 cycles per trial) for each spatial condition. All conditions employed a binary m-sequence of 63 bits encoded with black-background checkerboard (BB-CB) patterns, i.e., the encoding represented "1" with a checkerboard pattern and "0" with a black flash. Each condition assessed a specific spatial frequency of the stimuli, which refers to the size of the squares within a checkerboard-like stimulus, measured in cycles (pairs of squares of two alternative colors) per degree of visual angle (c/º). A total of 8 conditions were examined: C001 (0 c/º), C002 (0.15 c/º), C004 (0.3 c/º), C008 (0.6 c/º), C016 (1.2 c/º), C032 (2.4 c/º), C064 (4.79 c/º), and C128 (9.58 c/º). The stimuli and the arrangement of lags are shown in Figure 1(B). Online selections were made using a 3×3 command matrix (chance level of 11.11%). For further details, please see Fernández-Rodríguez *et al.* (2023) [7].

METHODS

Paradigm: In both datasets, the circular shifting paradigm was employed, which relies on using shifted versions of a pseudorandom sequence to encode individual commands, ensuring that only the original sequence needs to be calibrated. Consequently, it is imperative for the sequence to demonstrate minimal autocorrelation, thereby facilitating subsequent decoding [2]. Maximal length sequences (i.e., m-sequences), represent pseudo-random temporal series characterized by nearly optimal autocorrelation properties. These sequences are generated employing linear-feedback shift registers (LFSR). The characteristics of m-sequences are determined by three main factors: the base p, denoting the quantity of different events (e.g., $p = 2$ for binary m-sequences: events 0 and 1); the order r, indicating the number of LFSR taps; and the generator polynomial expressed within a Galois Field of p elements, GF(p), which defines the arrangement of the LFSR taps [5]. In addition to conforming to various mathematical constraints, the length of a m-sequence exactly equals $N = p^r - 1$ bits, repeating cyclically [5]. The larger the m-sequence, the greater the number of commands that can be encoded with it.

Signal processing: During the calibration stage, participants are instructed to focus on a single command encoded by the original m-sequence (without delay) for a duration covering k cycles (i.e., repetitions of the same m-sequence). Initially, the EEG signal undergoes preprocessing using a filter bank comprising three bandpass filters (ranging from 1 to 60 Hz, 12 to 60 Hz, and 30 to 60 Hz) and a notch filter set at 50 Hz [5, 7]. Two versions of the EEG response are subsequently computed for each signal: (1) concatenated epochs, denoted as $\boldsymbol{A} \in \mathbb{R}^{[kN_s \times N_c]}$; and (2) epochs averaged over the k cycles, denoted as $\boldsymbol{B} \in \mathbb{R}^{[N_s \times N_c]}$. Here, N_s represents the number of samples per cycle, and N_c represents the number

Published by
Verlag der Technischen Universität Graz

10.3217/978-3-99161-014-4-041

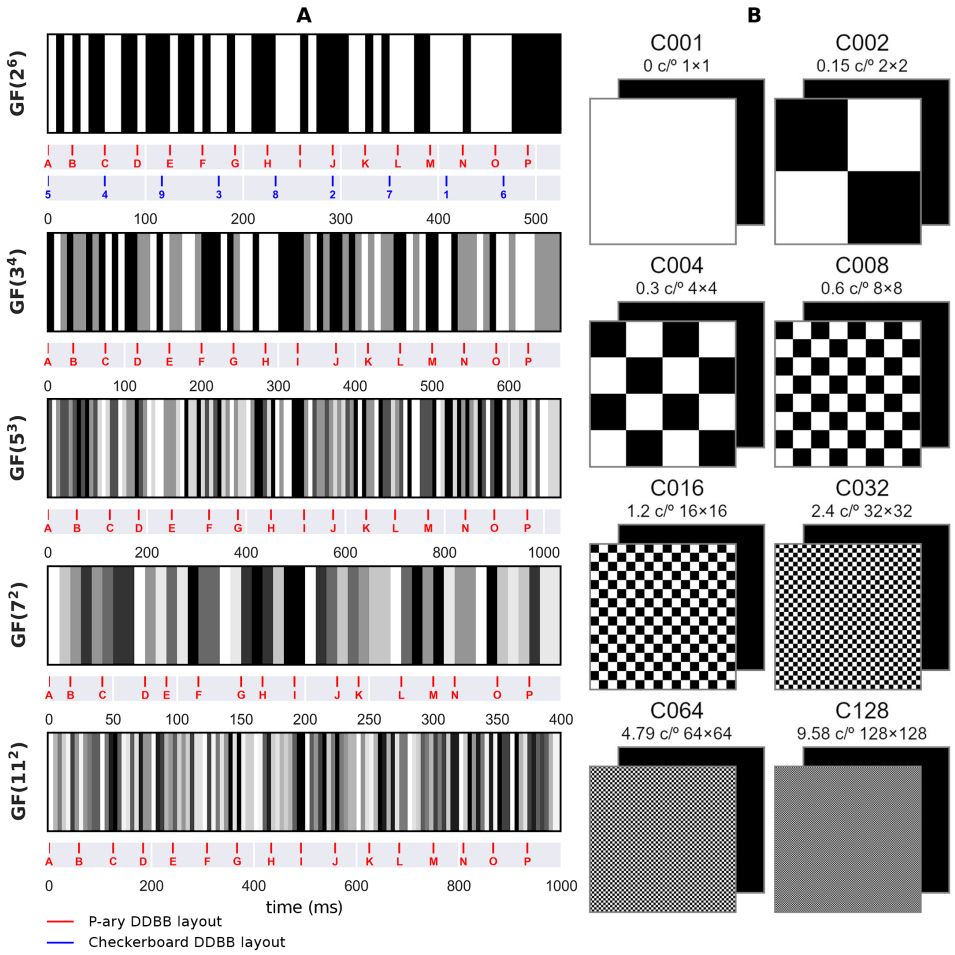

Figure 1: Stimuli details for both databases. (A) Gray encoding of each p-ary m-sequence over time, depicting associated lags for each command in the p-ary m-sequence database (shown in red) and checkerboard database (shown in blue). (B) Binary patterns of the black-background checkerboard (BB-CB) stimulus for the eight distinct spatial frequencies assessed in the checkerboard database. Note that all patterns (event 1) were coupled with a flickering monochromatic black square (event 0).

of channels. Subsequently, a canonical correlation analysis (CCA) is utilized to train the spatial filter $\boldsymbol{\omega}_b$ that maximizes the correlation between the projected versions of $\boldsymbol{A}$ and $\boldsymbol{B}$. In this process, $\boldsymbol{B}$ is replicated k times to match the dimensions of $\boldsymbol{A}$. The main template (i.e., for the command without delay) is established by projecting the averaged signal using the spatial filter $\boldsymbol{\omega}_b$, resulting in $\boldsymbol{x}_0 = \boldsymbol{B}\boldsymbol{\omega}_b$. Templates for the other commands are then generated by cyclically shifting this main template based on their respective delays. Following this procedure, $N_t \times 3$ templates, each for a command and filtered signal, are obtained, where N_t indicates the number of commands in the online stage. Therefore, $N_t = 16$ for the p-ary m-sequences database, and $N_t = 9$ for the checkerboard database. Calibration epochs with a standard deviation three times greater than the average standard deviation of all epochs were excluded before training the CCA [5, 7]. During the online mode, a similar approach is employed to determine the command the user is focusing on in real-time. The EEG signal undergoes preprocessing, and individual epochs are averaged and projected using the spatial filter $\boldsymbol{\omega}_b$. The correlation between the resulting projection and all templates is then computed, yielding $\hat{\boldsymbol{\rho}} \in \mathbb{R}^{N_t \times 3}$ values. After averaging across the filtered signals, $\boldsymbol{\rho} \in \mathbb{R}^{N_t}$ is obtained. The selected command corresponds to the one that produces the highest correlation value, identified as $\arg\max_i(\boldsymbol{\rho})$ [5, 7].

RESULTS

To understand how the duration of the calibration period affects the system's final performance, we (1) selected a specific number of calibration cycles k, (2) trained the model as outlined in the methods section, and (3) predict the outcome of the test trials and extract accuracy and ITR while varying the number of online cycles. The parameter k was systematically increased until the entire calibration dataset was utilized for each database, i.e., $k \in [1, 300]$. Figures 2 and 3 depict the grand-averaged accuracy across subjects for each condition and dataset. This accuracy is presented as a function of the number of calibration cycles k and the number of online cycles. The amount of calibration data is expressed in both the number of cycles and duration in seconds. As depicted, a

Published by
Verlag der Technischen Universität Graz

10.3217/978-3-99161-014-4-041

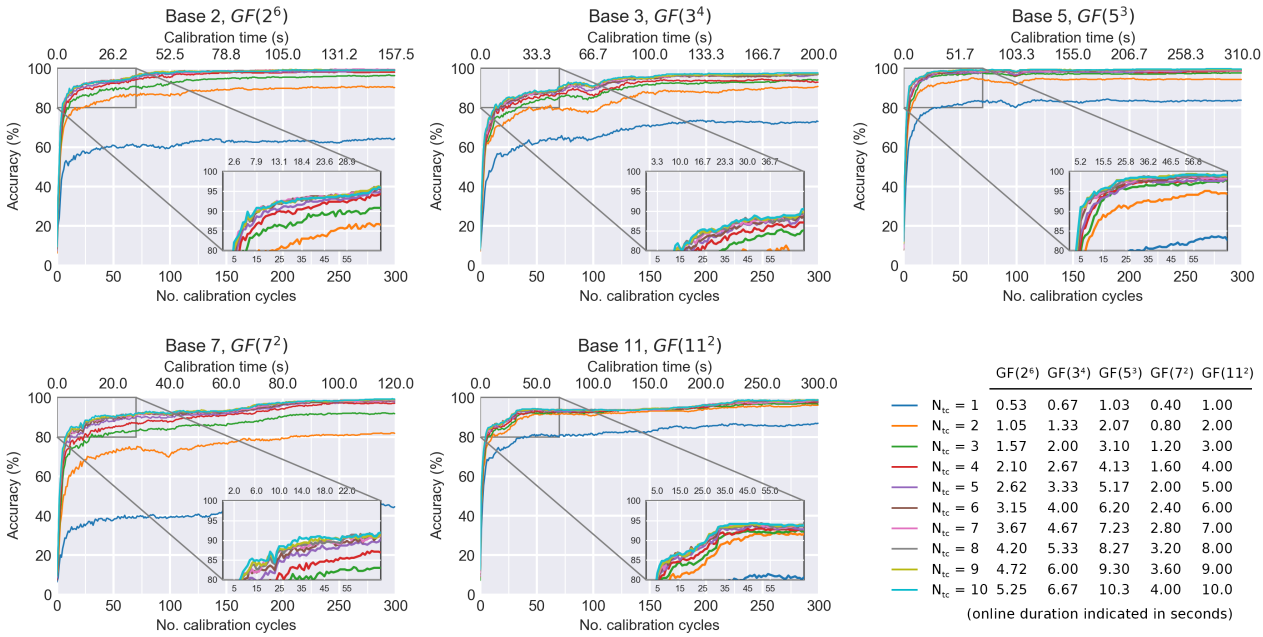

Figure 2: Grand-averaged accuracy across subjects for the p-ary m-sequences database as a function of the number of calibration cycles and the number of online cycles. The x-axis illustrates the quantity of calibration data utilized to train the model, expressed in both the number of cycles (bottom axis) and duration in seconds (top axis). Each curve represents a distinct number of online cycles (i.e., the length of the test epoch). Each plot corresponds to a different base. Chance level was 6.25%

Table 1: Analysis of plateau performance on the p-ary m-sequences database.

		Base 2, $GF(2^6)$			**Base 3,** $GF(3^4)$			**Base 5,** $GF(5^3)$			**Base 7,** $GF(7^2)$			**Base 11,** $GF(11^2)$		
	N_{oc}	2	5	10	2	5	10	2	5	10	2	5	10	2	5	10
	cal. (s)	74.55	9.45	5.78	96.00	37.33	28.67	19.63	10.33	5.17	-	24.40	12.40	34.00	27.00	24.00
0.9M	acc. (%)	89.45	89.84	89.84	88.09	87.89	87.89	90.04	91.02	91.02	-	89.65	89.84	89.06	89.45	89.06
	ITR (bpm)	177.3	71.53	35.76	135.3	53.90	26.95	91.25	37.31	18.66	-	93.47	46.94	92.24	37.22	18.45
	cal. (s)	-	34.12	31.50	-	76.00	52.00	62.00	22.73	11.37	-	73.60	65.20	195.0	47.00	37.00
0.95M	acc. (%)	-	94.73	94.34	-	92.97	92.97	95.12	95.51	94.92	-	94.53	94.53	93.95	93.95	94.14
	ITR (bpm)	-	79.91	39.60	-	60.45	30.22	102.4	41.34	20.39	-	104.4	52.21	103.0	41.21	20.70
	cal. (s)	-	-	109.2	-	-	175.3	-	-	276.9	-	-	118.8	-	-	237.0
1M	acc. (%)	-	-	99.22	-	-	97.66	-	-	99.80	-	-	99.41	-	-	98.83
	ITR (bpm)	-	-	44.61	-	-	33.73	-	-	23.06	-	-	58.88	-	-	23.17

N_{oc} indicates the number of online cycles, M the maximum accuracy for each base, "cal" the duration of the calibration in seconds, "acc." the accuracy in %, and "ITR" the information transfer rate in bits per minute. This analysis unveils the minimum calibration duration necessary to achieve 90%, 95%, and 100% of the maximum accuracy for each base, provided that such accuracy can be attained with each number of online cycles.

performance plateau is generally observed across all conditions. Tables 1 and 2 summarize the minimum calibration duration required to achieve 90%, 95%, and 100% of the maximum accuracy for each condition and database. Results are provided for varying numbers of online cycles. If that accuracy cannot be achieved with a particular number of online cycles, it is denoted with a hyphen.

DISCUSSION

As expected, the longer the calibration duration, the greater the accuracy achieved, regardless of the p-ary m-sequence or the spatial frequency of the BB-CB stimuli. While all conditions reached a performance plateau after a specific number of calibration cycles, independently of the number of online cycles, the slope (learning curve) appears to be dependent on the database or condition.

In the p-ary m-sequences database, all conditions achieved an average accuracy higher than 97% when using the maximum calibration duration. Overall, it is evident for all conditions that at least 2 online cycles are required to reach suitable performance. However, the performance plateau varied among them, indicating a trade-off between calibration duration and final performance. Specifically, $GF(5^3)$ and $GF(2^6)$ exhibited higher accuracy with less calibration duration, followed by $GF(11^2)$, $GF(7^2)$, and $GF(3^4)$. Considering an intermediate number of 5 online cycles, the 95th percentile of maximum accuracy (all above 92%) was achieved by using the following calibration durations, as shown in Table 1: 22.73 s for $GF(5^3)$, 34.12 s for $GF(2^6)$, 47.00 s for $GF(11^2)$, 65.20 s for $GF(7^2)$, and 76.00 s for $GF(3^4)$. These configurations also yielded ITRs above 40 bpm in all cases, i.e. maximum of 104.1 bpm for $GF(7^2)$, and minimum

Published by
Verlag der Technischen Universität Graz

10.3217/978-3-99161-014-4-041

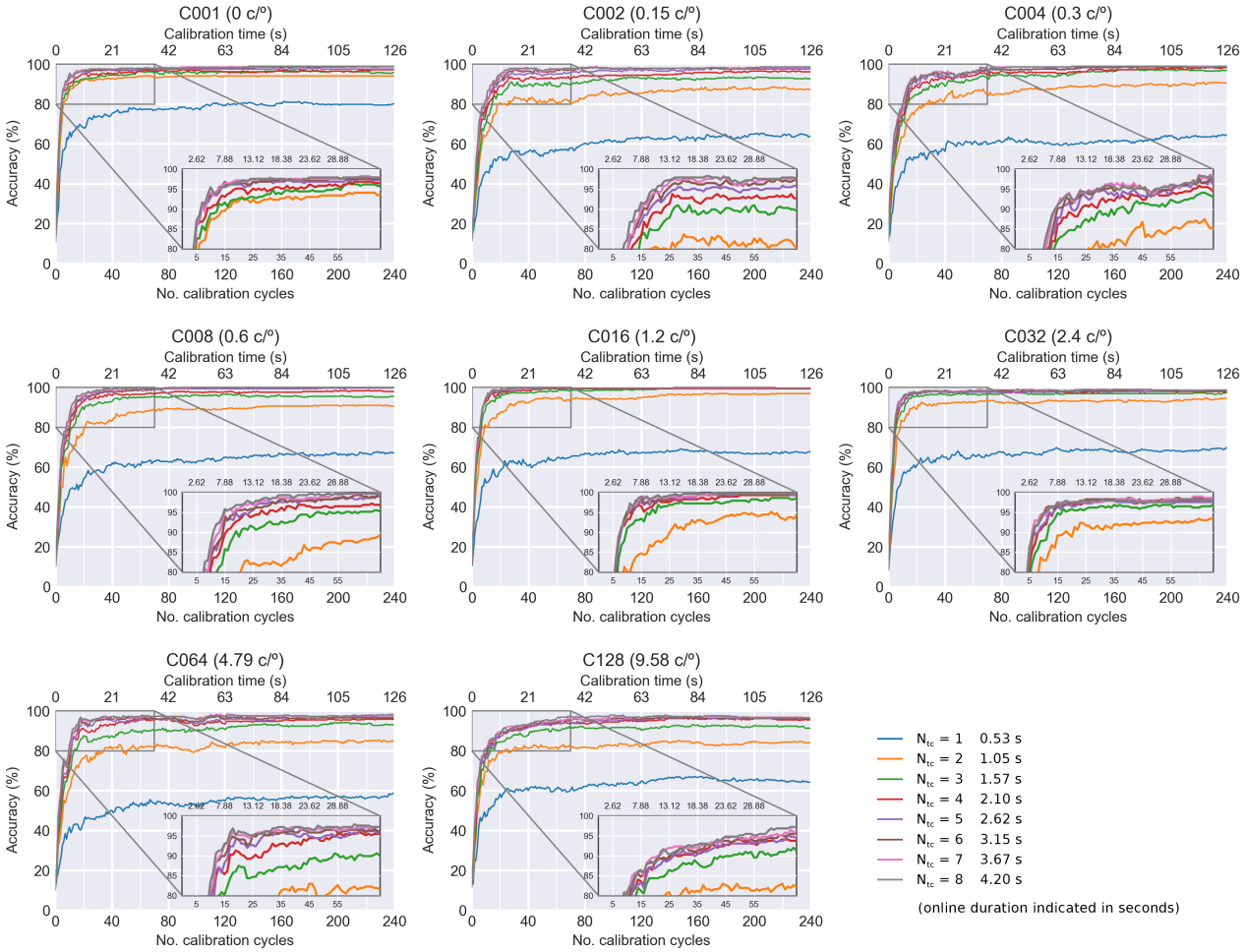

Figure 3: Grand-averaged accuracy across subjects for the checkerboard database as a function of the number of calibration cycles and the number of online cycles. The x-axis illustrates the quantity of calibration data utilized to train the model, expressed in both the number of cycles (bottom axis) and duration in seconds (top axis). Each curve represents a distinct number of online cycles (i.e., the length of the test epoch). Each plot corresponds to a different spatial frequency. Chance level was 11.11%.

Table 2: Analysis of plateau performance on the checkerboard database.

		C001 (0 c/°)		**C002 (0.15 c/°)**		**C004 (0.3 c/°)**		**C008 (0.6 c/°)**		**C016 (1.2 c/°)**		**C032 (2.4 c/°)**		**C064 (4.79 c/°)**		**C128 (9.58 c/°)**	
	N_{oc}	5	8	5	8	5	8	5	8	5	8	5	8	5	8	5	8
0.9M	cal. (s)	3.67	3.67	9.45	6.83	8.93	7.35	7.88	5.78	4.20	4.20	3.67	3.67	7.88	6.30	12.07	9.45
	acc. (%)	90.97	91.67	89.93	89.58	90.97	89.93	92.71	90.28	90.63	90.97	89.58	91.67	88.19	90.62	88.89	88.19
	ITR (bpm)	73.37	46.58	71.67	44.44	73.37	44.79	76.31	45.14	72.80	45.86	71.11	46.58	68.91	45.50	70.00	43.07
0.95M	cal. (s)	6.83	5.25	13.12	9.45	14.70	12.07	12.60	7.88	5.25	5.78	6.30	5.25	9.97	7.88	23.10	18.90
	acc. (%)	94.10	95.49	94.10	94.10	94.79	94.44	95.14	95.83	95.14	97.22	95.14	94.79	94.10	93.06	93.06	93.06
	ITR (bpm)	78.76	50.83	78.76	49.23	80.03	49.62	80.68	51.25	80.68	52.98	80.68	50.02	78.76	48.07	76.91	48.07
1M	cal. (s)	-	71.92	-	44.10	-	68.25	124.95	31.50	-	19.43	-	71.92	-	32.02	-	71.92
	acc. (%)	-	98.96	-	98.61	-	98.96	100.00	100.00	-	100.00	-	98.96	-	97.92	-	97.92
	ITR (bpm)	-	55.37	-	54.86	-	55.37	91.43	57.14	-	57.14	-	55.37	-	53.89	-	53.89

N_{oc} indicates the number of online cycles, M the maximum accuracy for each base, "cal." the duration of the calibration in seconds, "acc." the accuracy in %, and "ITR" the information transfer rate in bits per minute. This analysis unveils the minimum calibration duration necessary to achieve 90%, 95%, and 100% of the maximum accuracy for each base, provided that such accuracy can be attained with each number of online cycles.

of 41.21 bpm for GF(11^2). Nevertheless, the tradeoff between calibration/online selection duration and performance makes it difficult to select any specific configuration. For instance, in GF(2^6), it is feasible to calibrate with only 9.45 s, albeit at the cost of reducing the average accuracy to 89.84% and utilizing 2.62 s of online selection duration (at 71.53 bpm). Conversely, an impressive ITR of 177.3 bpm (at 89.45%) can be attained with an online selection duration of only 1.05 s by employing a calibration duration of 74.55 s. To sum up, all p-ary m-sequences prove capable of achieving above 90% mean accuracy through various configurations of calibra-

Published by
Verlag der Technischen Universität Graz

10.3217/978-3-99161-014-4-041

tion and online durations.

Regarding the checkerboard database, all spatial frequency conditions displayed similar performing plateaus. Once again, two online cycles are necessary to attain a practical level of control over the system. Note that condition C001 (0 c/º) is analogous to GF(2^6), and its superior performance may stem from the fact that the checkerboard database comprises only 9 commands instead of 16 [5, 7]. For 5 online cycles (2.62 s), all conditions demonstrated more than 93% accuracy and 76 bpm. Condition C016 stands out by achieving 95.15% accuracy and 80.68 bpm using only 5.25 s of calibration. Extending the calibration duration to 19.43 s and the online cycles to 8 (4.20 s), C016 attains 100% accuracy and 57.14 bpm. While we emphasize C016, similar behaviors are observed for C008 and C032, as indicated in Table 2. Generally, calibrations lasting between 3.67–12.07 s are sufficient to achieve accuracies around 88%-90% for all conditions, where C128 likely exhibits the poorest results.

It is evident that there exists a four-variable tradeoff involving calibration duration, online selection duration, system performance, and user comfort. Although all conditions can provide high-speed and high-performance BCIs, the performance plateau varies among them. The total number of commands also plays a significant role in interpreting these results. In conclusion, performance levels around 95% accuracy and 80 bpm can be readily attained with calibration durations ranging of 6–35 s and online selections of 2–3 s for binary m-sequences. Higher bases (i.e., $p > 2$) would lead to increased user comfort, as suggested by Martínez-Cagigal *et al.* (2023) [5], albeit at the cost of longer calibration periods. Concerning spatial frequencies, C016, followed by C008, emerged as the BB-CB stimuli associated with higher comfort scores [7]. Ultimately, the choice of configuration would depend on the functional requirements of the BCI system.

CONCLUSION

To our knowledge, this is the first study to examine the impact of the calibration phase on circular shifting paradigms for c-VEP-based BCIs. Regardless of the p base of the code or the spatial frequency of the BB-CB stimuli, all conditions can achieve high-speed and high-performance BCIs with sufficient calibration. We identified a tradeoff between calibration duration, online selection duration, performance, and user comfort. Performance levels nearing 95% accuracy and 80 bpm can be reached with calibrations lasting 6–70 s. While achieving over 95% accuracy with approximately 5 s of calibration and a selection duration of 2.62 s is possible with binary m-sequences, we stress the importance of selecting a configuration based on the requirements of the final BCI system, such as target performance and user comfort.

ACKNOWLEDGMENTS

This research has been developed under the grants TED2021-129915B-I00, PID2020-115468RB-I00 and PDC2021-120775-I00 funded by MCIN/AEI/10.13039/501100011033 and ERDF; under project ‘0124_EUROAGE_MAS_4_E’ (‘Cooperation Programme Interreg VI-A Spain-Portugal POCTEP 2021–2027’) funded by ‘European Commission’ and ERDF; and by CIBER-BBN through ‘Instituto de Salud Carlos III’ co-funded with ERDF funds.

REFERENCES

[1] Wolpaw J, Wolpaw EW. Brain-computer interfaces: principles and practice. OUP USA (2012).
[2] Martínez-Cagigal V, Thielen J, Santamaría-Vázquez E, Pérez-Velasco S, Desain P, Hornero R. Brain–computer interfaces based on code-modulated visual evoked potentials (c-VEP): a literature review. Journal of Neural Engineering. 2021;18(6):061002.
[3] Ladouce S, Darmet L, Torre Tresols JJ, Velut S, Ferraro G, Dehais F. Improving user experience of SSVEP BCI through low amplitude depth and high frequency stimuli design. Scientific Reports. 2022;12(1):1–12.
[4] Gembler FW, Rezeika A, Benda M, Volosyak I. Five Shades of Grey: Exploring Quintary m -Sequences for More User-Friendly c-VEP-Based BCIs. Computational Intelligence and Neuroscience. 2020;2020.
[5] Martínez-Cagigal V, Santamaría-Vázquez E, Pérez-Velasco S, Marcos-Martínez D, Moreno-Calderón S, Hornero R. Non-binary m-sequences for more comfortable brain–computer interfaces based on c-VEPs. Expert Systems with Applications. 2023;232(June):120815.
[6] Shirzhiyan Z *et al.* Introducing chaotic codes for the modulation of code modulated visual evoked potentials (c-VEP) in normal adults for visual fatigue reduction. PLoS ONE. 2019;14(3):1–29.
[7] Fernández-Rodríguez Á, Martínez-Cagigal V, Santamaría-Vázquez E, Ron-Angevin R, Hornero R. Influence of spatial frequency in visual stimuli for cVEP-based BCIs: evaluation of performance and user experience. Frontiers in Human Neuroscience. 2023;17.
[8] Spüler M, Rosenstiel W, Bogdan M. Unsupervised BCI Calibration as Possibility for Communication in CLIS Patients? In: Proceedings of the Fifth International Brain-Computer Interface Meeting 2013. 2013, 10–12.
[9] Thielen J, Marsman P, Farquhar J, Desain P. From full calibration to zero training for a code-modulated visual evoked potentials brain computer interface. Journal of Neural Engineering. 2021;18(5):56007.
[10] Stawicki P, Volosyak I. cVEP Training Data Validation—Towards Optimal Training Set Composition from Multi-Day Data. Brain Sciences. 2022;12(2).
[11] Santamaría-Vázquez E *et al.* MEDUSA©: A novel Python-based software ecosystem to accelerate brain-computer interface and cognitive neuroscience research. Computer Methods and Programs in Biomedicine. 2023;230(107357).

Published by
Verlag der Technischen Universität Graz